

**DESIGN AND SIMULATION OF HIGH LINEARITY  
AND STABILITY OPERATIONAL AMPLIFIER  
CIRCUITRY FOR AMPEROMETRIC SENSOR**

**By**

**ANGIE LEE SHIN SHIN**

**A Dissertation submitted for partial fulfilment of the requirement for  
the degree of Master of Science (Microelectronic Engineering)**

**August 2017**

## **ACKNOWLEDGEMENT**

First and foremost, I would like to express my gratitude to my academic supervisor, Assoc. Prof. Dr Asrulnizam Bin Abd Manaf from Collaborative Microelectronic Design Excellence Center (CEDEC), Universiti Sains Malaysia (USM) who has provided the guidance and assisted me to obtain knowledge in this field, at the same time, helping me to promptly complete my master research studies.

As part of my research project, I had the opportunity to spend time in Collaborative Microelectronic Design Excellence Center (CEDEC) Penang to conduct my research. I would like to thank Ruhaifi Abdullah Zawawi from CEDEC for his support and guidance throughout my project. He has provided me with numerous brilliant idea and guidance in completing my master research.

Last but not least, I would like to thank my company, Intel Microelectronics (M) Sdn Bhd for providing the opportunity and my manager for encouraging me to further study in USM. Without the full support from the management team, I would not have a chance to enroll in the master program.

## TABLE OF CONTENT

	Page
ACKNOWLEDGEMENT	ii
TABLE OF CONTENT	iii
LIST OF TABLE	vii
LIST OF FIGURES	viii
LIST OF ABBREVIATION	xii
ABSTRAK	xiii
ABSTRACT	xvi
CHAPTER 1 INTRODUCTION	1
1.1 Introduction	1
1.2 Problem Statement	3
1.3 Research Objectives	3
1.4 Scope and Limitation	4
1.5 Thesis Structure	5
CHAPTER 2 LITERATURE REVIEW	7
2.1 Introduction	7
2.2 Electrochemical Sensor Review	9
2.2.1 Faradaic Current	10
2.2.2 Overpotential	10
2.2.3 Amperometric Sensors	11
2.3 Amplified Redox Sensor (ARS)	13

2.3.1 Direct Amplified Redox Sensor	13
2.3.2 Direct Amplifier Redox Sensor with BJT	14
2.3.3 Direct Amplifier Redox Sensor with BJT and Diode	15
2.4 Potentiostat Control Configuration	16
2.4.1 Potential Control	17
2.4.1(a) Grounded WE Configuration	17
2.4.1(b) Grounded CE Configuration	17
2.4.2 Current Measurement	19
2.4.2(a) Current Measurement with Transimpedance Amplifier	19
2.4.2(b) Two-electrode Electrochemical Sensor with Current Conveyor	20
2.4.2(c) Current Measurement with Resistor at WE	21
2.4.2(d) Current Measurement with Resistor at CE	22
2.5 Potentiostat Topologies	23
2.5.1 Single-ended Potentiostat	23
2.5.1(a) Control Part	24
2.5.1(b) Amplify Part	24
2.5.2 Fully Differential Potentiostat	25
2.5.2(a) Wide Swing Cascoded Current Mirror	27
2.5.2(b) Fully Differential Transimpedance Amplifier	28
2.6 Three-electrode Amperometric Sensors with Current Mirror Based Potentiostat	30
2.6.1 Current Mirror Based Potentiostat	30

2.6.2 Improved Current Mirror Based Potentiostat	31
2.6.3 Current Mirror Based Potentiostat (Oxidation Current)	32
2.7 Summary	34
CHAPTER 3 RESEARCH METHODOLOGY AND IMPLEMENTATION	35
3.1 Introduction	36
3.2 Sensor Block	40
3.2.1 Sensor Block Circuit Design Process and Methodology	40
3.3 Amplifier Block	44
3.3.1 Amplifier Block Circuit Design Process and Methodology	44
3.4 Full Potentiostat System Circuit Integration and Performance	50
3.4.1 Full Potentiostat System Circuit Integration	50
3.4.2 DC gain and Phase Margin	52
3.4.3 Slew Rate	54
3.4.4 Power Supply Rejection Ratio (PSRR)	55
3.4.5 Total Power Consumption	56
3.5 Potentiostat System Layout Design	57
3.5.1 Potentiostat Layout Design Process and Methodology	57
3.6 Potentiostat System Post-layout Simulation	58
3.7 Summary of Research Methodology and Implementation	59
CHAPTER 4 RESULTS AND DISCUSSION	60
4.1 Introduction	60
4.2 Sensor Block	61
4.3 Amplifier Block	64

4.4 Full Potentiostat System Circuit Integration and Performance	68
4.4.1 Full Potentiostat System Circuit Integration	68
4.4.2 Gain and Phase Margin	70
4.4.3 Slew Rate	73
4.4.4 Power Supply Rejection Ratio (PSRR)	74
4.4.5 Total Power Consumption	75
4.5 Potentiostat System Layout Design	76
4.6 Post-Layout Simulation Results	78
4.7 Summary of the Results and Discussion	79
CHAPTER 5 CONCLUSIONS AND FUTURE WORK	82
5.1 Conclusions	82
5.2 Future Work	83
REFERENCES	84
APPENDICES	87
APPENDIX A	87
APPENDIX B	88

## LIST OF TABLE

		Page
Table 2.1	Summary of the Different Design of Potentiostat System	34
Table 3.1	Sensor Block Components Parameter	44
Table 3.2	Amplifier Block Components Parameter	50
Table 4.1	Summary of the Potentiostat System Design Parameter	80

## LIST OF FIGURES

	Page	
Figure 2.1	Conceptual drawing of a Three-electrode Amperometric Electrochemical Sensor and a Potentiostat	8
Figure 2.2	Three-electrode Amperometric Sensor. (a) Schematic Representation. (b) Simplified electrical-equivalent model	12
Figure 2.3	(a) Basic measurement circuit (b) Results of the basic measurement unit with positive and negative current peaks	14
Figure 2.4	(a) BJT Based Amplifier Circuit (b) Measurements when the bias voltage applied to the BJT	15
Figure 2.5	(a) Measurement circuit with a BJT and a diode (b) Results of inserting a diode	16
Figure 2.6	Grounded WE Potential Control Circuit	18
Figure 2.7	Grounded CE Potential Control Circuit	18
Figure 2.8	Transimpedance Amplifier Current Measurement Circuit	20
Figure 2.9	Two-electrode Electrochemical Sensor with Current Conveyor	21
Figure 2.10	Current Measurement with Resistor WE	22
Figure 2.11	Current Measurement with Resistor CE	23
Figure 2.12	Single-ended Potentiostat Block Diagram	24
Figure 2.13	Fully-differential Potentiostat Building Blocks	25
Figure 2.14	Fully-differential Potentiostat Schematic	27



Figure 2.15	Fully Differential (a) Schematic of FD TIA (b) FD TIA Amplifier Circuitry	29
Figure 2.16	Common Mode Feedback (CMFB) Circuitry	29
Figure 2.17	Current Mirror Based Potentiostat System	31
Figure 2.18	Improved Current Mirror Based Potentiostat System	32
Figure 2.19	Current Mirror Based Potentiostat System (Oxidation Current) (a) $V_{out}$ with Reference to $V_{DD}$ (b) $V_{out}$ with Reference to $V_{DD}$	33
Figure 3.1	General Design Flows for the Potentiostat System	37
Figure 3.2	Full Potentiostat System	39
Figure 3.3	Single-ended Potentiostat System Block Diagram	39
Figure 3.4	Sensor Block Circuitry	41
Figure 3.5	Test bench circuit for Sensor Block	43
Figure 3.6	Original Transimpedance Amplifier Block Circuitry without Compensation Circuit	45
Figure 3.7	Original Transimpedance Amplifier Test bench Circuit without Compensation Circuit	46
Figure 3.8	Transimpedance Amplifier Block Circuitry with Compensation Circuit	48
Figure 3.9	Transimpedance Amplifier Test bench with Compensation Circuit	49
Figure 3.10	Full Potentiostat System Circuitry	51
Figure 3.11	Full Potentiostat System Test bench Circuit	52

Figure 3.12	Test bench Circuit to Determine Transimpedance Amplifier Design DC gain and Phase Margin	53
Figure 3.13	Test bench Circuit for the Potentiostat System to Determine the Slew Rate	54
Figure 3.14	Test bench Circuit for the Potentiostat System to Determine the Power Supply Rejection Ratio	56
Figure 4.1	Sensor Block Output When Low Bias Voltage was Applied	62
Figure 4.2	DC Analysis $V_{bias1}$ Swept from 0-2 V to get a Stable $V_{bias1}$	63
Figure 4.3	Sensor Block Output with default Transistors Width and Length	63
Figure 4.4	Sensor Block Output with Optimized Transistors Width and Length	64
Figure 4.5	DC Analysis on $V_{DD}$ Swept from 0-2 V for Amplifier	65
Figure 4.6	DC Analysis on $V_{DD}$ Swept from 0-2 V for Amplifier with Compensation Circuit	66
Figure 4.7	$V_{out2}$ having almost flat and constant value from $V_{DD}$ range of 1.65 V to 2 V	67
Figure 4.8	Swept $I_{sensor}$ to Measure $V_{out2}$	67
Figure 4.9	Potentiostat System $V_{out}$ with Response to the change of $V_{DD}$ at constant Input Sensor Current = 10 $\mu$ A	69
Figure 4.10	Potentiostat System $V_{out}$ with Response to the Change of the Input Sensor Current	69
Figure 4.11	DC Swept on $V_{bias}$ to Get a Correct $V_{bias}$ for the Amplifier	71
Figure 4.12	Transimpedance Amplifier Design DC Gain Result	72

Figure 4.13	Transimpedance Amplifier Design Phase Margin when Gain is 0 dB	72
Figure 4.14	Measurement of Input and Voltage Signals of the Potentiostat System with Square Wave Input Current	73
Figure 4.15	Slew Rate Measurement for the Potentiostat System	74
Figure 4.16	PSRR Measurement for Potentiostat System	75
Figure 4.17	Measured $I_{DD}$ at $V_{DD} = 1.8$ V and $R_f = 20$ k $\Omega$	76
Figure 4.18	Potentiostat System Die Size Measurement in X and Y	77
Figure 4.19	Pre-layout and Post-layout Simulation Results for Potentiostat Output Voltage	78

## LIST OF ABBREVIATION

ADC	Analogue to Digital Converter
SOC	System on Chip
IC	Integrated Circuit
TIA	Transimpedance Amplifier
FD	Fully Differential
SE	Single Ended
EMI	Electromagnetic Interference
CMOS	Complementary Metal Oxide Semiconductor
BJT	Bipolar Junction Transistor
VDD	Voltage Supply
SR	Slew Rate
PSRR	Power Supply Rejection Ratio
PM	Phase Margin
ARS	Amplified Redox Sensor
AE	Auxiliary Electrode
WE	Working Electrode
RE	Reference Electrode
CE	Counter Electrode
R	Resistor
C	Capacitor
SAR	Successive Approximation Register

**REKABENTUK DAN SIMULASI LITAR PENGUAT OPERASI DENGAN  
KESTABILAN DAN KELURUSAN TINGGI UNTUK PENDERIA  
AMPEROMETRIK**

**ABSTRAK**

Penderia redoks digunakan secara meluas untuk mengesan analit tertentu dalam larutan kimia terutamanya kepekatan larutan kimia. Penderia redoks mempunyai kelebihan pengesanan pelbagai ion dalam kawasan penderia dengan pengukuran dan menukar ke arus elektrik atau voltan. Walau bagaimanapun, kepekaan dan isyarat keluaran penderia akan menurun disebabkan oleh pengecilan kawasan penderia. Tesis ini membentangkan rekabentuk potentiostat yang dapat memproses arus penderia redoks yang kecil antara julat 0 hingga 10  $\mu\text{Amp}$  dengan keluaran yang lurus serta isyarat voltan yang telah dikuatkan untuk diintegrasikan dengan litar pertukaran analog ke digital (ADC). Potentiostat ini juga menghasilkan keluaran yang stabil apabila  $V_{DD}$  berubah secara dinamik dari lingkungan 1.65 V ke 2.0 V. Blok penderia dibina untuk model penderia redoks sebenar dan berupaya menukarkan isyarat secara lurus untuk keluaran. Blok penguat penggalangan direkabentuk untuk menguatkan penukaran arus ke voltan secara lurus. Potentiostat yang direkabentuk telah mencapai gandaan arus terus (DC), margin fasa, kadar sl<sub>u</sub>, nisbah penolakan bekalan kuasa dan jumlah penggunaan kuasa adalah 8.34 dB, 107.7°, 3.8 V/ $\mu\text{s}$ , 26.82 dB dan 1.5208 mW. Rekabentuk susun atur untuk sistem potentiostat merangkumi keluasan kawasan acuan ialah 2983.54  $\mu\text{m}^2$  dengan keluaran voltan potentiostat adalah dari 894 mV ke 1.094 V.

**DESIGN AND SIMULATION OF HIGH LINEARITY AND STABILITY  
OPERATIONAL AMPLIFIER CIRCUITRY FOR AMPEROMETRIC SENSOR**

**ABSTRACT**

Redox sensor is widely used to detect certain analytes of a chemical solution especially concentration of a chemical solution. Redox sensor has advantages of detection of multiple ions inside a sensing areas by measurement and represent it in electrical current or voltage. However, sensitivity and output signal of sensor decreases due to miniaturization of sensing area. This thesis presents a design of a potentiostat that is able to process the redox sensor small output signal in the range of 0 A to 10  $\mu$ A and has a linear and amplified voltage signal for integration with analogue digital conversion (ADC) circuit. It provides a stable output when the voltage supply,  $V_{DD}$  is dynamically changing from the range of 1.65 V to 2.0 V. Sensor block is constructed to model the real redox sensor and must be able to linearly convert current signal to the output. Then, the amplifier blocks which is a transimpedance amplifier, is designed to perform current-to-voltage conversion and linearly amplify the redox sensor current signal to voltage. The designed potentiostat is able to achieve DC gain, phase margin, slew rate, power supply rejection ratio and total power consumption were 8.34 dB, 107.7°, 3.8 V/ $\mu$ s, 26.82 dB and 1.5208 mW, respectively. The layout design for the full potentiostat systems is done with the die area of 2983.54  $\mu$ m<sup>2</sup> and the range of potentiostat output voltage is from 894 mV to 1.094 V.

# CHAPTER 1

## INTRODUCTION

### 1.1 Introduction

Electrochemical sensor is a sensor that transforms the effects of the electrochemical interaction of analytes and electrode into a measurable signal. Electrode system was used in various electrochemical approaches like potentiometric, voltammetric and amperometric. One of the widely use application of electrochemical sensor is redox sensor which detects oxidation and reduction reaction of chemical solution.

Miniaturization of sensor devices for integration with an integrated circuit is indirectly causing sensing areas to decrease and hence causing the sensor output signal to drop significantly. This small output signal is undesirable outcome as sensing devices have other various application which involve integration with other design that only accept certain range of input voltage such as analogue to digital convertor (ADC) circuits.

Current method is by using a operational amplifier to amplify the output signal from the sensor. Based on Takahashi, S. *et al.*, designed amplified redox sensor (ARS) with directly amplified redox sensor for on-chip chemical analysis by using BJT and

diode which allows the flow of positive and negative current at the same time [1]. However, the demand for increased functionality and system size minimization will force these system-on-chip (SoC) designs to be implemented in advanced CMOS processes.

Based on Wang, W. S. *et al.*, single-ended transimpedance amplifier (TIA) was implemented by connecting a negative feedback resistor to prevent non-constant transconductance (gm) effect of the transistor for high linearity [2]. However, the result is not stable and the linearity is low whenever  $V_{DD}$  is varied. Hence, amplifier design which has high linearity and stable across a range of  $V_{DD}$  is required to support portable device application.

Ahmadi, M. M. *et al.* presented new topology which is the current mirror based potentiostat which uses a current mirror to generate a mirrored image of sensor current instead of direct using the sensor current from redox. This topology has the advantages of low power consumption, smaller die size, and lower noise but it behave non-linearly due to current mirror mismatches. [3].

Steven M. Martin *et al.* designed potentiostat based on a fully differential transimpedance amplifier (TIA) [4, 5]. The gain is double of single ended, but the design is more complex and requires more components which affect the total power consumption. The study on how to make amplification linearly on small current signal of redox sensor output and also the conversion of the current signal to voltages with a potentiostat is an important study for integration with an ADC design.



## 1.2 Problem Statement

Output signal of an electrochemical sensor will decrease or get very small when sensing area of the sensor is decreased due to miniaturization of sensor devices for integration of sensor to an integrated circuit (IC). A small output signal from a sensor is an unfavorable outcome especially when integration of sensor to analog-to-digital converter (ADC) circuit is an important application as ADC can only take in a certain range of input voltage.

Boosting electrochemical sensor small output signal to a readable range for ADC circuit is crucial in the field of electro-chemical sensor study. One of the common ways is to design an amplifier that is well integrated with the electrochemical sensor. For sensor output signal in current form, the current to voltage conversion is essential for integration to ADC since it only takes voltage as input.

## 1.3 Research Objectives

The objectives of this research:

- To model the redox sensor by constructing a cascoded current mirror circuit that is able to linearly produce current for redox sensor output signal in the range of 0 A to 10  $\mu$ A.

- To design and simulate the potentiostat system circuit with high linearity and stability that made up of a transimpedance amplifier (TIA) to perform current-to-voltage conversion for redox sensor signal which is independent of dynamic  $V_{DD}$  changes in the range of 1.65 V to 2.0 V.

#### **1.4 Scope and Limitation**

The scope of this research works is to study and design a full potentiostat system that able to take-in small current signal from redox sensor range from 0 A to 10  $\mu$ A and then perform current-to-voltage conversion. The small current signal is also linearly amplified and observed at potentiostat output terminal.

This design uses Silterra 0.18  $\mu$ m process with voltage supply of range is within 1.65 V to 2.0 V where the output voltage is stable and not fluctuated due to power supply changes and operates at room temperature of 27° C. After circuit design is done, the physical layout design will be performed for the potentiostat system and finally followed by post-layout simulation on potentiostat system.

## 1.5 Thesis Structure

This thesis is structured in five chapters. Brief explanation of each chapter is given as below:

Chapter 2, Literature Review explains in detail on review of the field of study of electrochemical sensor with the main focus on the electrochemistry of amperometric sensor, operation of a potentiostat, existing published potentiostat topologies, new potentiostat topologies, current mirror design techniques that being used for amperometric sensor, circuit design techniques and concept that being used in Amplifier Redox Sensor (ARS) for chemical solution analysis.

Chapter 3, Research Methodology and Implementation will present the method and work flow that being used to represent the potentiostat design that able to take-in the redox sensor small current signal from 0 A to 10  $\mu$ A. Detail explanation on the cascoded current mirror design, and transimpedance amplifier design that form the full potentiostat system and also physical layout design methodology will be presented in this chapter.

Chapter 4, Results and Discussion will present the results of the cascoded current mirror design, and the performance of the transimpedance amplifier that forms the potentiostat systems with post-layout simulation results.

Chapter 5, Conclusions and Future Work concludes the thesis on the data and findings that has been presented in the previous chapter to come out with the potentiostat design and lays the groundwork for the proposed potentiostat systems.

## CHAPTER 2

### LITERATURE REVIEW

#### 2.1 Introduction

Chemical analysis is heavily used in scientific fields, such as medical science, environmental and biological study. A redox sensor can sense the type of ion and do the measurement to the concentration of ions. The output current signal of a redox sensor is directly proportional to the concentration of the solution and the size. The output current of the redox sensor decreases as the sensing area decreases. Large sensing area is needed to measure solution with low concentration and this leads to inducing a large parasitic capacitance at the interface with the electrode [1].

Amperometric sensor is one of the popular methods to detect analytes which use a potentiostat to control the electrode cells when conducting analysis on the electrochemical solutions. Potentiostat integration into CMOS chip helps in cost saving, system size and form a system on chip (SOC) when combined with other applications [2].

It consists of three electrodes which are the working electrode (WE) which is the place where the electrochemical reaction happens, the reference electrode (RE) is used to

measure potential quantity present in WE electrode, and the counter electrode which used to supply current require for the reduction and oxidation of the chemical solutions. A high input impedance is used to prevent current goes through and affected the voltage at RE [2].

Figure 2.1 illustrate a three electrode amperometric sensor which combined a working electrode (WE) for an electrochemical reaction takes place, a reference electrode (RE), which is used to measure the solution potential and a counter electrode (CE) that supply the current required for electrochemical reaction at WE. Potentiostat is used to control the potential difference between WE and RE at a desired cell potential by injecting the proper amount of current into CE [3].

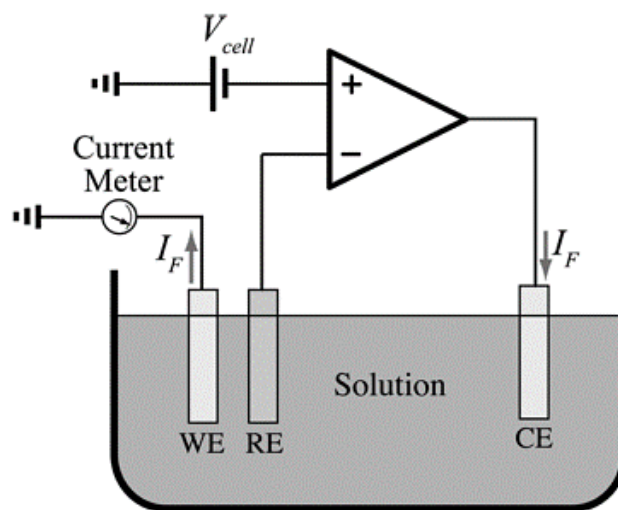


Figure 2.1: Conceptual drawing of a Three-electrode Amperometric Electrochemical Sensor and a Potentiostat [3]

Due to the demand to increase functionality and system size minimization, it force these system-on-chip (SoC) designs to be implemented in advanced CMOS processes. The range of chemical analysis is limited by the scaled supply voltage in this process. The drive voltages of amperometric chemical sensors which do not varied with electrode size but determined by the reduction/oxidation (redox) potentials of the analytes had been studied [4].

This chapter will be focused on the discussion of the study of electrochemistry of amperometric sensor, operation of the potentiostat, the potentiostat topologies, new potentiostat topologies such as single-ended (SE) potentiostat and fully differential (FD) potentiostat, current mirror circuit design techniques that being implemented for potentiostat. The circuit design techniques and concept for amplifier redox sensor (ARS) for the study of reduction and oxidation reaction of chemical solution will also be discussed.

## **2.2 Electrochemical Sensor Review**

In this section, electrochemistry study on faradaic current, overpotential and electrochemical sensor theory on amperometric sensor are discussed.

### 2.2.1 Faradaic Current

With the absence of an externally applied voltage in equilibrium, a potential based on the ratio of the solution's chemical species will be developed in a single polarizable electrode resting in the solution. The system is forced to be out of equilibrium whenever an overpotential is supplied to this electrode. Hence, reduction and oxidation (redox) reactions take place, which is explained below as shown in Equation 2.1.



where  $O$  is the species oxidized form,  $n$  is the number of electrons per molecule oxidized or reduced,  $e^{-}$  is an electron, and  $R$  is the species reduced form. This results in a faradaic current at the electrode surface. The measured faradaic current,  $I_f$  also represents the specific ion concentration [5].

### 2.2.2 Overpotential

In a chemical solution, the overpotential is compulsory for redox reactions to take place in a given chemical solution. Analytical measurement of the chemical solution cannot take place if an insufficient overpotential is supplied to the electrode. For example, in a platinum electrode, the chemical liquid tends to decompose for overpotential



which is more positive than 1.5 V and more negative than -1.5V. Overpotential which is outside of  $|1.5V|$  is a limitation, hence this lead to development of potentiostat system for low voltage operation [5].

### 2.2.3 Amperometric Sensors

Conventional sensor is a three-electrode amperometric cell which consist of auxiliary electrode (AE), reference electrode (RE), and working electrode (WE) as shown in Fig. 2.2(a). The faradaic reaction happens at the WE. The RE draws zero current and it is a non-polarizable electrode that tracks the chemical solution potential. Hence, the potential between the electrode and chemical solution causing faradaic reaction to take place which is given by Equation 2.2.

$$V_{WE} - V_{RE} = V_{cell} \quad (2.2)$$

where  $V_{WE}$  and  $V_{RE}$  are the potentials at the WE and RE respectively. The potential of the solution is set via secondary redox reactions and enable by AE which sources the current required for the faradaic reaction to take place. Figure 2.2(b) shows an electrical equivalent model of a three-electrode amperometric sensor [5].

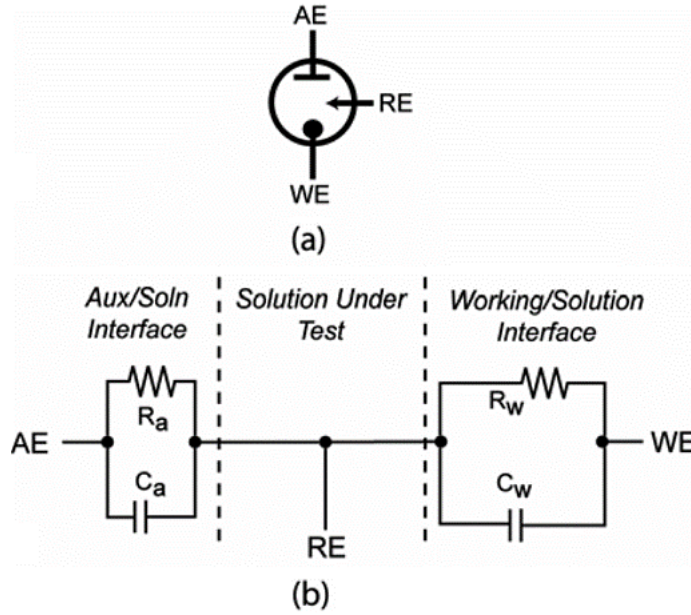


Figure 2.2: Three-electrode Amperometric sensor (a) Schematic representation (b) Simplified electrical-equivalent model [5]

Solution impedances typically are small and negligible.  $R_A$  and  $R_W$  are the faradaic resistances,  $C_A$  and  $C_W$  are the double-layer capacitances associated with the AE and WE, respectively which are given by Equation 2.3.

$$C_X = K_C A_X \quad (2.3)$$

where  $C_X$  is the electrode capacitance,  $A_X$  is the electrode area, and  $K_C$  is a constant value of 0.36.  $R_W$  is defined in Equation 2.4 where  $I_f$  is the faradaic current and  $R_W$  must be recalculated based on the measured  $I_f$ , if  $V_{cell}$  changes [5].

$$R_W = \frac{V_{cell}}{I_f} \quad (2.4)$$

## 2.3 Amplified Redox Sensor (ARS)

Amplified redox sensor (ARS) is required to measure small redox currents which consist of a sensing electrode and a working electrode together with an amplifier. There are many types of combination which can be use in order for the redox sensor output to be amplified. One of the direct method is to use a bipolar transistor (BJT) for the amplification. The drawback of an ARS with bipolar transistor is that it limits the flow of a positive or negative current with respect to the type of transistor for rectification [1].

### 2.3.1 Direct Amplified Redox Sensor

Figure 2.3(a) shows the basic redox potential and current measurement circuit with three electrodes which are the working electrode (WE), the reference electrode (RE), and the counter electrode (CE). The WE is used for current measurement, the CE is used to apply voltage to the chemical solution, and the RE is used for voltage measurement. Figure 2.3(b) shows the concentration result of the substance which obtained from the absolute value of each current peak that called “redox potential” which can be expressed in Equation 2.5.

$$I_p = (2.69 \times 10^5)n^{3/2}AD^{1/2}Cv^{1/2} \quad (2.5)$$

where  $I_p$  is the peak current,  $n$  is the electrons number involved,  $A$  is the WE area,  $D$  is the diffusion constant,  $v$  is the scan rate, and  $C$  is the bulk concentration. From Equation

2.5, the redox sensor current is directly proportional to the size of the sensing area and the ions concentration [1].

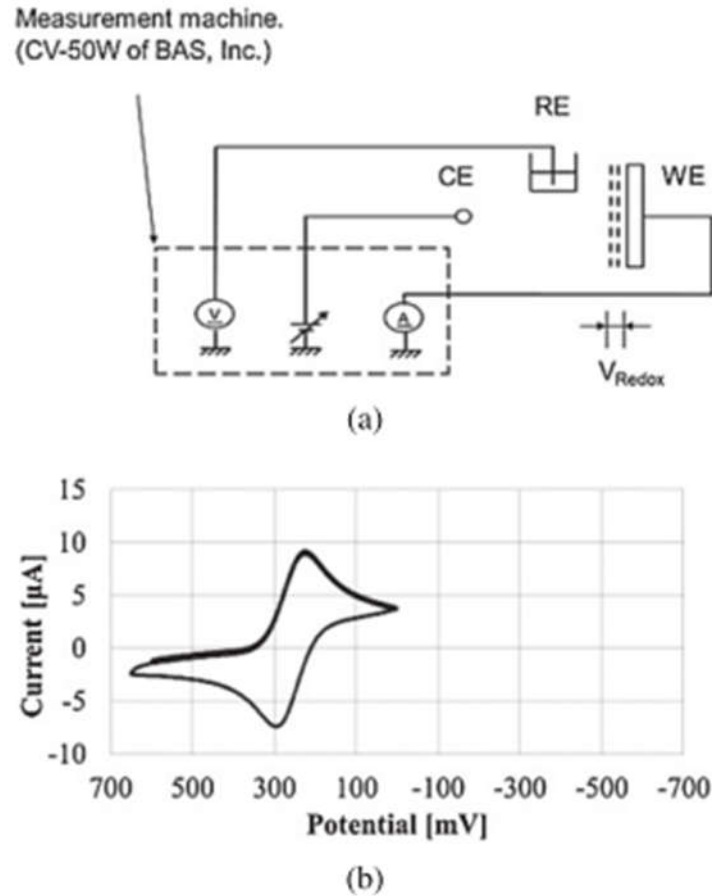


Figure 2.3: (a) Basic measurement circuit (b) Results of the basic measurement unit with positive and negative current peaks [1]

### 2.3.2 Direct Amplifier Redox Sensor with BJT

Figure 2.4(a) shows the WE is connected to the base of the BJT and the collector is connected to a bias voltage. The current flows through the emitter is then amplified and

measured. Due to the forward voltage  $V_{BE}$  of the BJT, the redox potential was expected to shift [1].

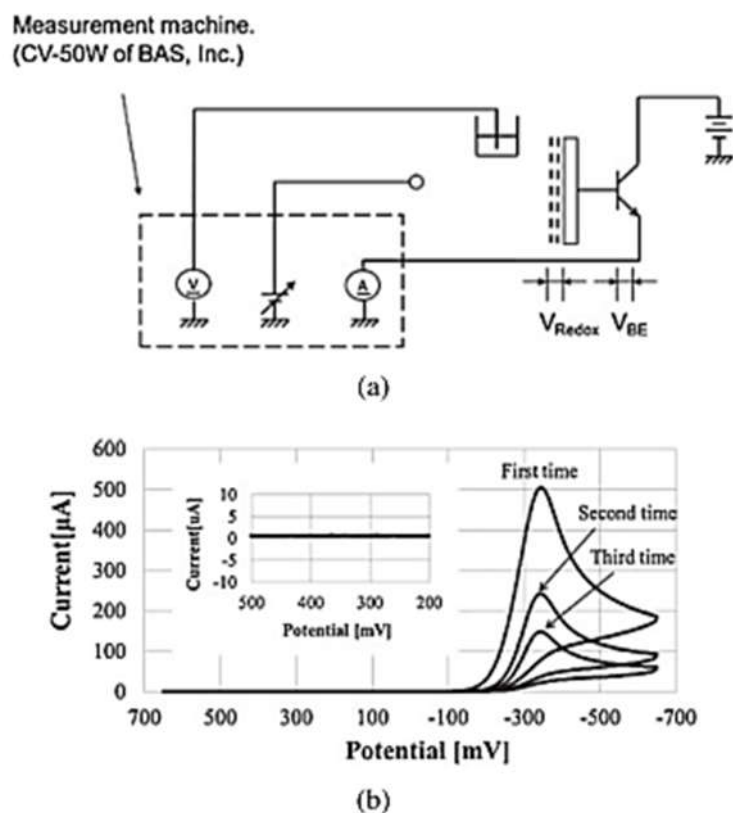


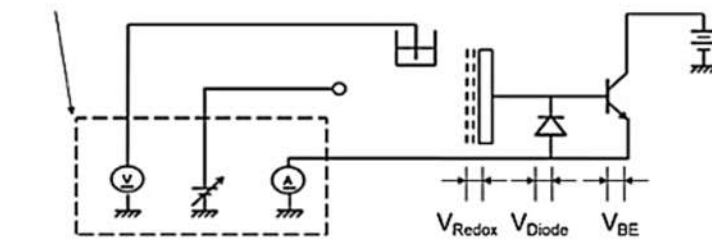
Figure 2.4: (a) BJT Based Amplifier Circuit (b) Measurements when the bias voltage applied to the BJT [1]

### 2.3.3 Direct Amplifier Redox Sensor with BJT and Diode

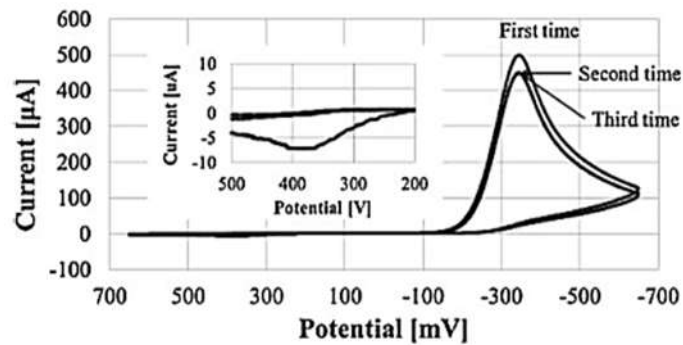
Figure 2.5(a) shows the measurement circuit configuration with a BJT and a diode. The advantage to insert a diode is to obtain both currents of reduction and oxidation without breaking the supply balance between both. Figure 2.5(b) shows the current signal

result by using emitter-to-base current, emitter current to base voltage characteristic of the BJT and diode current to voltage characteristics [1].

Measurement machine.  
(CV-50W of BAS, Inc.)



(a)



(b)

Figure 2.5: (a) Measurement circuit with a BJT and a diode (b) Results of inserting a diode [1]

## 2.4 Potentiostat Control Configuration

There is two fundamental operations of the circuit configurations, which is potential control and current measurement.

### 2.4.1 Potential Control

The value of the measurement points for the potential control configuration is by using CE grounded [6], WE grounded [7, 8] and virtual grounded WE. There is no direct connection to the real ground for virtual grounded CE, therefore, it is having risk to absorb noise from environment which causes significant noise levels at the TIA output terminal. It is also produces huge capacitive that causes inconsistent results to the control amplifier. The grounded counter electrode configuration is more complex and more components are required which makes it more vulnerable to common interference and mismatches [2].

#### 2.4.1(a) Grounded WE Configuration

Figure 2.6 shows the basic implementation of grounded WE configuration. WE is kept at the ground potential, and an operational amplifier, called the control amplifier, controls the cell current  $I_F$  such that the cell potential  $V_{cell}$  is kept at its desired preset potential  $E_i$  [3].

#### 2.4.1(b) Grounded CE Configuration

Busoni, L. *et al* had explored the grounded CE configuration as replacement for potential control configuration as shown in Figure 2.7 [6]. It has higher complexity and

more components are required which leads to more vulnerable to component mismatches. Grounded CE configuration potentially provides better current measurement if the WE connection could shield properly from external electromagnetic interference (EMI) [3].

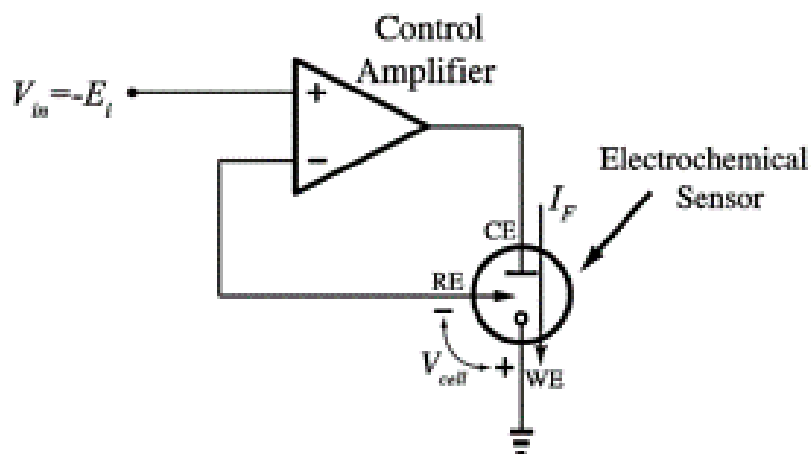


Figure 2.6: Grounded WE Potential Control Circuit [3]

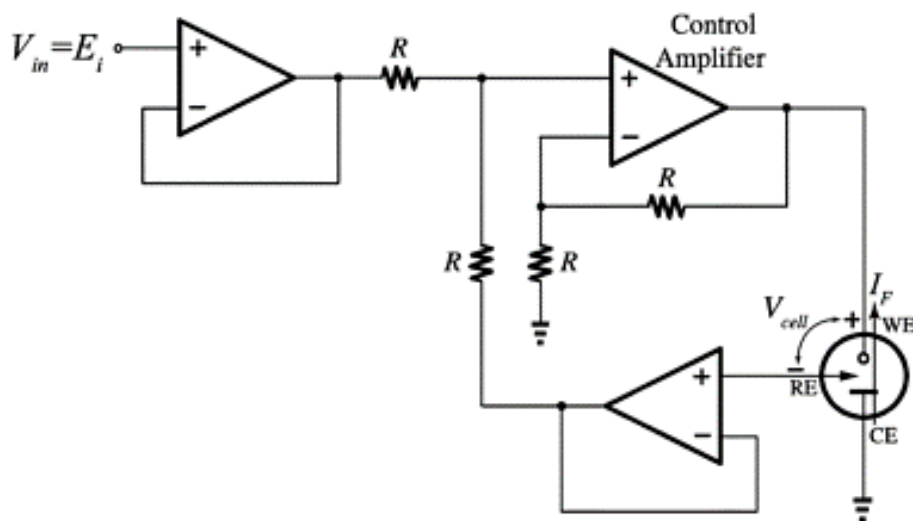


Figure 2.7: Grounded CE Potential Control Circuit [3]



## 2.4.2 Current Measurement

Current measurement approaches that had been used are readout current through WE and readout through CE. Readout current through WE offers more advantages over the second configuration. For example, by using the transimpedance amplifier that offers few currents measurement by altering resistor value for current measurement. The drawback is that it produces noise at the transimpedance amplifier output due to no physical connection between WE and the true ground. It also produces large capacitive components that affect the inductivity of the amplifier. Literatures [9-15] used two-electrode sensor current conveyor where the WE is at virtual ground and causes significant noise level [3].

For readout current through counter electrode, the three-electrode current conveyor had been used in [8] and [16] but there is the disadvantages due to saturated voltage and nonlinearity. The WE is at actual ground to prevent noise and interference. Ahmadi, M. M. *et al.* used current mirror conveyor as an option but the potentiostat behave non-linearly due to the current mirror mismatch [3].

### 2.4.2(a) Current Measurement with Transimpedance Amplifier

A transimpedance amplifier produce an output that is directly proportional to  $I_F$  as shown in Figure 2.8. This approach has a few advantages [17], [18] such as relatively simple as tiny current is measurable by altering the resistor,  $R_M$  [3].

However, it picks up noise from environmental as well as high frequency EMI when WE is not directly connect to an actual real ground and the potentiostat is not shielded properly. The noise passes through  $R_M$  is induced and create significant noise level at output of the TIA. Second drawback is that at high frequencies, the input impedance increases due to the roll-off in the open-loop gain of the TIA. Very large capacitive components generated due to the input impedance connected in series with the electrochemical cell [3].

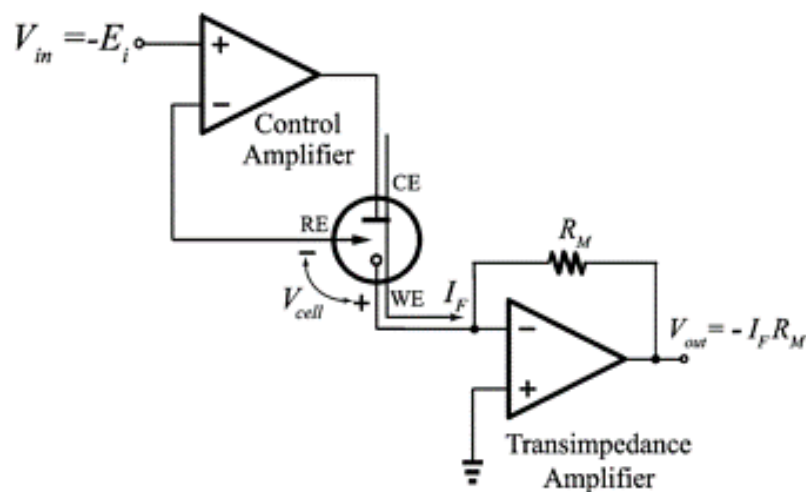


Figure 2.8: Transimpedance Amplifier Current Measurement Circuit [3]

#### 2.4.2(b) Two-electrode Electrochemical Sensor with Current Conveyor

Figure 2.9 shows a two electrode current conveyor approach for current measurement. The WE is connected to virtual ground and conveyed from WE to a node(X) which is high in impedance. It is capable to convert the sensor current to variables other than voltage, such as time and frequency.

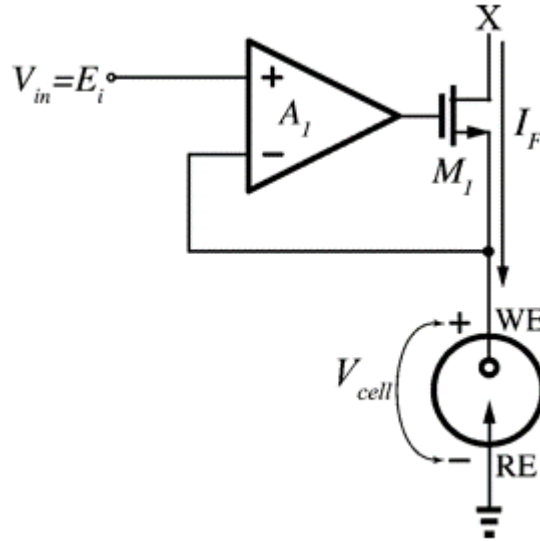


Figure 2.9: Two-electrode Electrochemical Sensor with Current Conveyor [3]

#### 2.4.2(c) Current Measurement with Resistor at WE

Figure 2.10 shows the current measurement approach by using resistor at the current path of WE, voltage across that resistor can be measured. The WE is not at the ground potential but it varied depending on  $I_F$ . Current is measured and feedback to the control amplifier for proper potential control. It has higher complexity than a conventional transimpedance amplifier (TIA) and more active and passive components are needed. The drawback is that it is more prompted to mismatch due to components, noise and interference issues. The advantages of this design that it is able to measure very small input current and voltage that are measured with reference to ground [3].

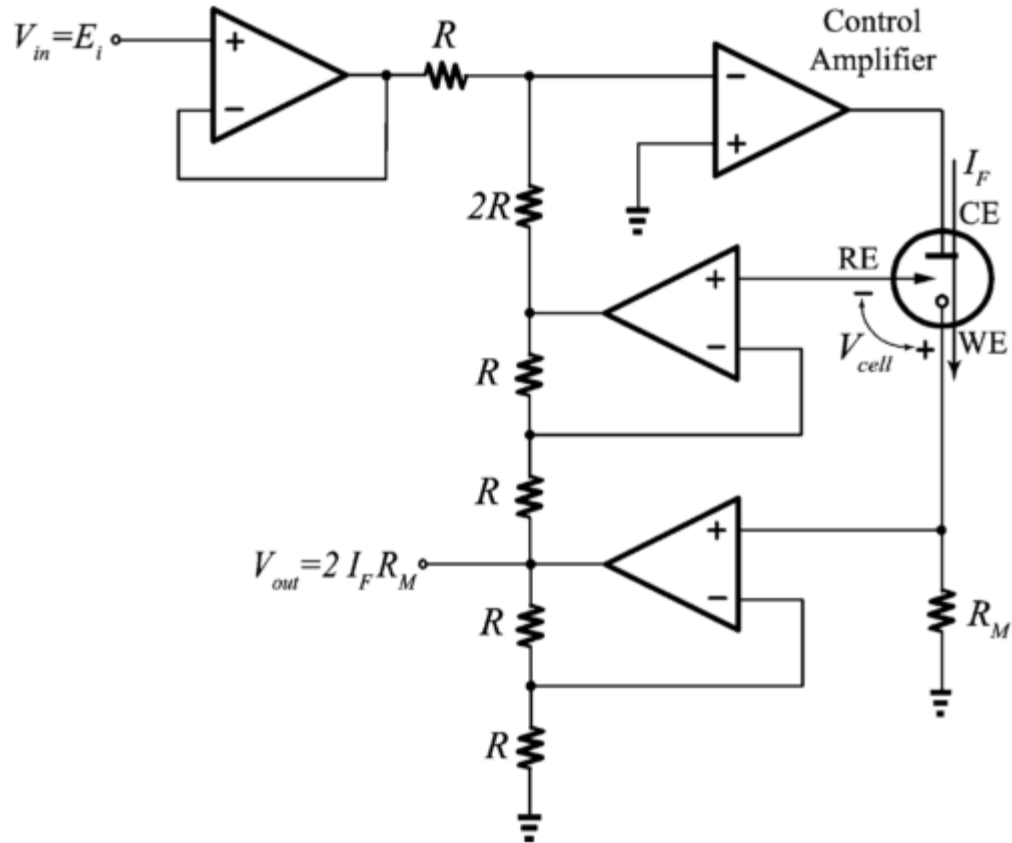


Figure 2.10: Current Measurement with Resistor WE [3]

#### 2.4.2(d) Current Measurement with Resistor at CE

Figure 2.11 shows the approach for current measurement by using a resistor at the current path of CE and followed by measurement of the voltage across that resistor. This approach has the drawback of mismatches in the components but the advantage of shielding from noise due to having WE connected to a real ground. Other advantages are it does not have the additional active component in the control feedback loop and having better stability compared to the previously mentioned design. The voltage and current are measured with reference to ground. Both configuration circuits suffer on the reduction

of the voltage swing range as the voltage drop across  $R_M$  increases with the increases of sensor current [3].

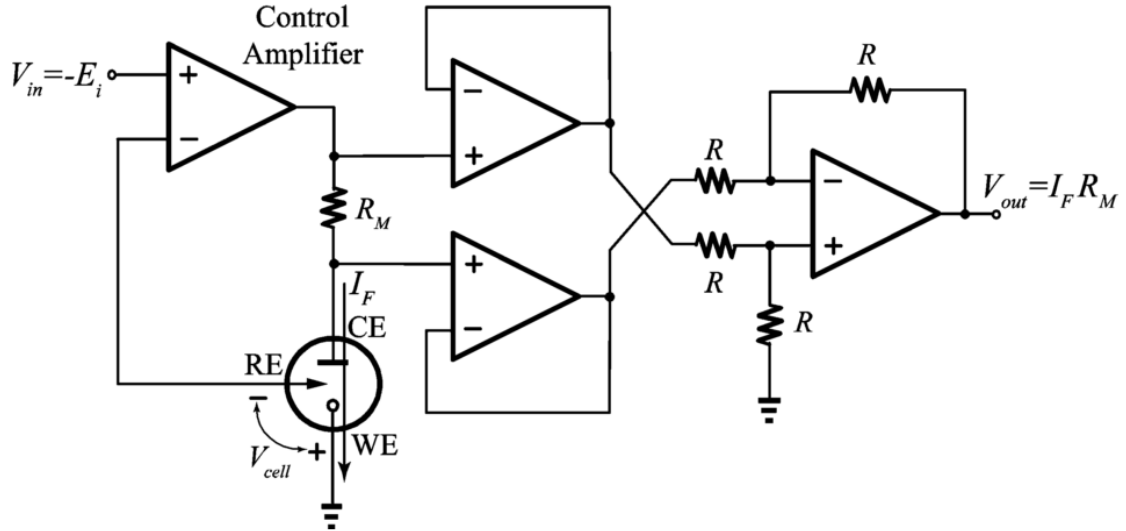


Figure 2.11: Current Measurement with Resistor CE [3]

## 2.5 Potentiostat Topologies

There is many ways of potentiostat such as single-ended and fully differential which can be explain in details next.

### 2.5.1 Single-ended Potentiostat

Figure 2.12 shows the single-ended potentiostat topology block diagram which consists of control part and the amplifying part. The details explanation of each functional block will be discuss below [2].

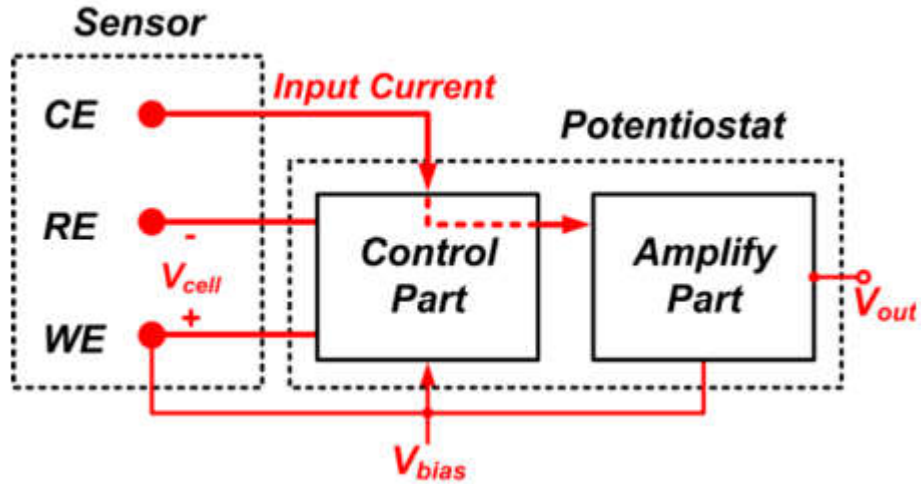


Figure 2.12: Single-ended Potentiostat Block Diagram [2]

### 2.5.1(a) Control Part

The main function of the control part is to maintain the potential level for the system where the voltage between WE and RE is forced to be the same as voltage bias ( $V_{bias}$ ). CE will be the drive or source input current to the control part of the system [2].

### 2.5.1(b) Amplify Part

The system current from CE is captured and current is converted to output voltage in amplify part. Current are blocking from flowing into the RE by connect RE directly to the input of the control part. The control amplifier output is connected to the gate of current mirror transistor instead of CE directly to avoid large capacitance of the counter